Potential Precursors to and Implications of Tropical Cyclone Passage: A Regional Climate Perspective

Ben Schenkel (bschenkel@fsu.edu) and Robert Hart (rhart@fsu.edu)
Department of Earth, Ocean, and Atmospheric Science, Florida State University

Introduction

While there are approximately 80–90 tropical cyclones (TCs) globally every year (Gray 1985; Frank and Young 2007), temporally integrated TC intensity metrics such as power dissipation exhibit significant interdecadal variability (Emanuel 2005). Explaining the variation of these intensity metrics appears to be fundamentally rooted in determining the relevance of TCs within the global energy cycle. While previous research has quantified the role of the large scale atmospheric heat transport processes (e.g Newton 1972; Trenberth and Caron 2001), there has been little attempt to determine the role of TCs within this framework. On local scales, TCs are known to be responsible for a net flux divergence of heat from the ocean surface to the thermocline via entrainment mixing and upwelling (e.g. Leipper 1967; Chang and Anthes 1978; Price 1981) and to the atmosphere through fluxes of latent and sensible heat. Determining whether these localized impacts on the aggregate are significant raises the question as to whether the general circulation would be substantially different if TCs did not exist? The following study seeks to quantify the interactions between TCs and their environment in space and time as a first step in answering these questions.

Methodology

In this study, storm-relative composites of raw and normalized anomalies are constructed using data from the NCEP Climate Forecast System Reanalysis (Saha et al. 2010). Normalized anomalies are calculated relative to an evolving climatology:

$$N = \frac{X - \mu}{\sigma} \qquad (1)$$

where N is the normalized anomaly, X is the raw variable, μ is the daily climatological mean, and σ is the daily climatological standard deviation. Both σ and μ have been smoothed with a 1–2–3–2–1 filter to reduce the contribution of features with time scales of less than one week. TCs within the western North Pacific equatorward of 36°N during the years 1982–2001 are chosen for study. The intensity and position of TCs are obtained from the JTWC best-track dataset (Chu et al. 2002). Composites are created by bilinearly interpolating each grid to a uniform resolution centered upon the best-track location of the TC for 60 days prior to 60 days after TC passage. Each reanalysis TC is then composited into one of three intensity bins according to its best-track intensity. Unless explicitly stated, the results presented here apply to category 3–5 TCs.

Quantifying Interactions Between Tropical Cyclones and Their Environment

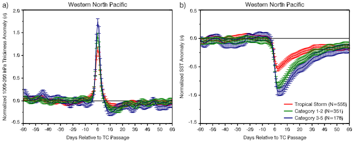

Figure 1: Time series of 500 km by 500 km box averaged composites of (a) normalized 1000–200 hPa thickness anomalies (σ) and (b) normalized SST anomalies (σ) for TCs stratified according to their best-track intensity. The red line represents tropical storms, the green line represents category 1–2 TCs, and the blue line represents category 3–5 TCs. The error bars denote the standard error of the mean. The number of distinctly named cases for each intensity bin is noted in the legend.

Extending the Analysis of the Anomalies into Four Dimensions

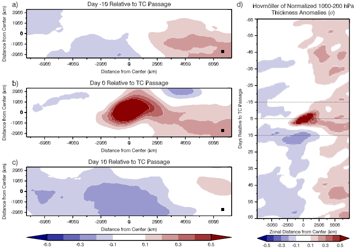

Figure 2: Plan view of normalized 1000–200 hPa thickness anomalies (σ) for (a) Day -10 relative to TC passage, (b) Day 0 relative to TC passage, and (c) Day 10 relative to TC passage within the composite domain. The solid square in (a), (b), and (c) represents the center position over which box-averaged vertical cross-sections are computed for Figure 5 and the latitude band over which the Hovmöllers in Figure 6 are calculated over. (d) Hovmöller diagram of normalized 1000–200 hPa thickness anomalies (σ) in the zonal direction relative to the composite domain center. Anomalies are averaged over a meridional distance extending from -500 km to 500 km from the latitude band located at the composite domain center. The three dotted lines in (d) correspond to the days plotted in the plan view plots in (a), (b), and (c).

Examining the Vertical Structure of the Environmental Anomalies

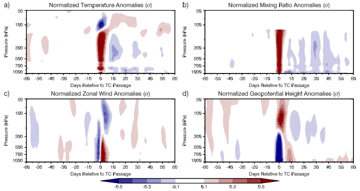

Figure 3: Time series of the vertical cross-section of (a) normalized temperature anomalies (σ), (b) normalized mixing ratio anomalies (σ), (c) normalized zonal wind anomalies (σ), and (d) normalized geopotential height anomalies (σ) averaged over a 500 km by 500 km box located at the composite domain center.

Existence of Forcings on Multiple Scales Following Tropical Cyclone Passage

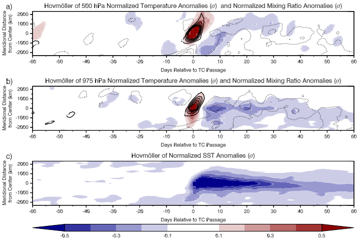

Figure 4: Hovmöller diagram of (a) 500 hPa normalized temperature anomalies (σ, shaded) and normalized mixing ratio anomalies (σ, contoured every 0.1σ), (b) 975 hPa normalized temperature anomalies (σ, shaded) and normalized mixing ratio anomalies (σ, contoured every 0.1σ), and (c) normalized SST anomalies (σ) in the meridional direction relative to the composite domain center. Anomalies are averaged over a zonal distance extending from -500 km to 500 km from the longitude band located at the composite domain center.

Potential Precursors to and Implications of Tropical Cyclone Passage: A Regional Climate Perspective

Ben Schenkel (bschenkel@fsu.edu) and Robert Hart (rhart@fsu.edu)
Department of Earth, Ocean, and Atmospheric Science, Florida State University

Influence of Large Scales on Environmental Pre-Conditioning

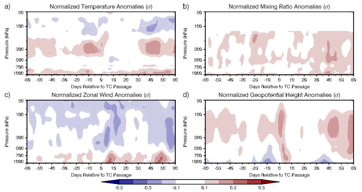

Figure 5: As in Figure 3, but for a 500 km by 500 km box centered on the east side of the domain at the position denoted by the filled square in Figure 2.

Determining the Relevance of the Anomalies Through Energy Considerations

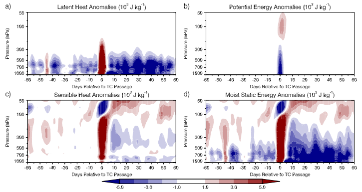

Figure 7: As in Figure 3, but for (a) potential energy anomalies (J kg^{-1}), (b) latent heat anomalies (J kg^{-1}), (c) sensible heat anomalies (J kg^{-1}), and (d) moist static energy anomalies (J kg^{-1}).

Discussion

The results of this study show that prior to the passage of a TC, the atmosphere is both thermodynamically and dynamically destabilized. An east-west dipole of normalized anomalies is found primarily at low levels with a warmer, moister environment on the east side of the domain and colder, drier anomalies to the west. Westerly low level zonal wind anomalies are noted to persist in the southeastern quadrant of the domain consistent with the presence of anomalous cyclonic vorticity. The magnitude of these anomalies increases most strongly starting around 10 days prior to TC passage. The possibility remains that these anomalies are ENSO driven given their qualitative resemblance. While the passage of the TC results in the cooling and drying of the atmosphere maximized over the cold SST wake of the TC, the composite domain experiences a cooling and drying of the troposphere beyond the scales of the TC. The westerly zonal wind anomalies are also observed to intensify and propagate eastward in the weeks following TC passage. The large spatio-temporal response in the thermodynamic and dynamic fields surrounding the time of TC passage agrees with previous work (Sobel and Camargo 2005). Calculation of moist static energy anomalies reveal that the negative 100–200 hPa thickness anomalies following TC passage are primarily attributable to the drying of the lower and middle troposphere. Using composited moist static energy anomalies from each basin, a total annual value of 0.01 PW can be attributed to recurving TCs within the eastern North Pacific, North Atlantic, and western North Pacific. Given that peak Northern Hemisphere energy transports are on the order of 5.0 PW (Trenberth and Caron 2001), these calculations indicate that TCs play a more relevant role in heat transport in the ocean as opposed to the atmosphere. These computations suggest that TCs can be both active and passive players in the global energy cycle.

Evolution of the Large Scale Anomalies in Space and Time

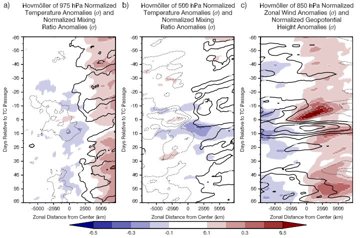

Figure 6: Hovmöller diagram of (a) 975 hPa normalized temperature anomalies (σ, shaded) and normalized mixing ratio anomalies (σ, contoured every 0.1σ), (b) 500 hPa normalized temperature anomalies (σ, shaded) and normalized mixing ratio anomalies (σ, contoured every 0.1σ), and (c) 850 hPa normalized zonal wind anomalies (σ, shaded) and normalized geopotential height anomalies (σ, contoured every 0.1σ) in the zonal direction relative to the latitude band of the filled square in Figure 2. Anomalies are averaged over a meridional distance extending from -500 km to 500 km from the latitude band coincident with the filled square.

Comparing the Integrated Impact of Tropical Cyclones on Their Environment

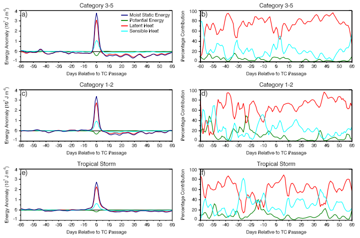

Figure 8: Time series of 500 km by 500 km box averaged potential energy anomalies (J m^{-2}), latent heat anomalies (J m^{-2}), sensible heat anomalies (J m^{-2}), and moist static energy anomalies (J m^{-2}) for (a) category 3–5 TCs, (c) category 1–2 TCs, and (e) tropical storms. The blue line represents moist static energy, the green line represents potential energy, the red line represents latent heat, and the cyan line represents sensible heat. Time series of the relative percentage contribution of the magnitude of each component for (b) category 3–5 TCs, (d) category 1–2 TCs, and (f) tropical storms.

Acknowledgements and References

This research is supported by NASA Headquarters under the NASA Earth and Space Science Fellowship Program Grant 10-Earth10R-0036 and NSF Grant ATM-0842618. We acknowledge the FSU HPC facility and staff for contributions to the results presented in this poster.

Camargo, S. and A. Sobel, 2005: Western North Pacific Tropical Cyclone Intensity and ENSO. *J. Climate*, **18**, 2996–3006.
Chang, S. and R. Anthes, 1978: Numerical Simulations of the Oceans Nonlinear, Baroclinic Response to Translating Hurricanes. *J. Phys. Oceanogr.*, **8**, 468–480.
Chu, J., C. Sampson, A. Levine, and E. Fukada, 2002: The Joint Typhoon Warning Center Tropical Cyclone Best-Tracks, 1945–2000. *Naval Research Laboratory, Reference Number NRL/MR/7540-02-16.*
Emanuel, K., 2001: Contribution of tropical cyclones to meridional heat transport by the oceans. *J. Geophys. Res.*, **106**, 14,771–14,781.
Emanuel, K., 2005: Increasing Destructiveness of Tropical Cyclones Over the Past 30 Years. *Nature*, **436**, 686–688.
Frank, W. and G. Young, 2007: The interannual variability of tropical cyclones. *Mon. Wea. Rev.*, **135**, 3587–3598.
Gray, W., 1985: Tropical cyclone global climatology. *WMO Tech. Doc.*, **72**.
Leipper, D., 1967: Observed Ocean Conditions and Hurricane Hilda, 1964. *J. Atmos. Sci.*, **24**, 182–186.
Newton, C., 1972: Meteorology of the Southern Hemisphere. *Meteor. Monog.*, **1**.
Price, J., 1981: Upper ocean response to a hurricane. *J. Phys. Oceanogr.*, **11**, 153–175.
Saha, S. and Coauthors, 2010: The NCEP climate forecast system reanalysis. *Bull. Amer. Meteor. Soc.*, **91**, 1015–1057.
Trenberth, K. and Caron J.M., 2001: Estimates of meridional atmosphere and ocean heat transports. *J. Climate*, **14**, 3433–3443.